Universitat Autònoma de Barcelona

**Departament de Química**

**Facultat de Ciències**

# New Functional Ligands for the Preparation of Photoactive Nanoparticle-Based Materials

**Laura Amorín Ferré**

**Ph.D. Thesis**

**Ph.D. in Chemistry**

**2014**

Supervisors:

Dr. José Luis Bourdelande Fernández

Dr. Félix Busqué Sánchez

Dr. Jordi Hernando Campos

# CHAPTER IV

# Aggregates of Quantum Dots via Strain-Promoted Azide-Alkyne Cycloaddition

In this chapter the development of a new methodology for the preparation of discrete heteroaggregates of covalently-tethered colloidal quantum dots is described. Our approach relies on the functionalization of the semiconductor nanoparticles with ligands bearing azide and cyclooctyne groups, which can undergo Cu-free, strain-promoted azide-alkyne cycloaddition under standard ambient conditions. As a first step towards the fabrication of future nanophotonic devices, we aimed herein to demonstrate the viability and potential of this synthetic strategy to conduct the controlled assembly of quantum dots.

Manuscript in preparation

.

# IV.1. INTRODUCTION

Colloidal quantum dots (QD) are a few nanometer-sized semiconductor particles, composed of an inorganic crystalline core coated with organic ligands, which are synthesized and suspended in solution.[1] While different organic functionalities can be used as stabilizers (e.g. thiols, carboxylic acids, amines, phosphine oxides), their inorganic core must consist of binary, or even ternary, mixtures of type II-VI (e.g. ZnS), III-V (e.g. InP) and IIV-VI (e.g. PbSe) semiconductors. QDs present some unique optoelectronic properties due to quantum confinement effects that can be modulated by tailoring their composition, size and shape. In particular, we are interested in these systems because they exhibit high, stable and spectrally narrow photoluminescence, which can be finely tuned along the electromagnetic spectrum. As an example, Figure IV-1 shows the emission ranges of QDs of different chemical compositions, which span from the UV to the IR regions.[2] Among them, our attention has specifically focused on CdSe QDs in this thesis, because their photoluminescence falls in the visible spectrum.[3]

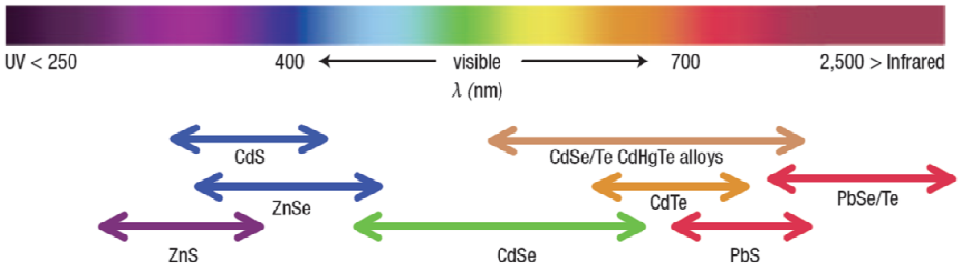


**Figure IV-1.** Emission ranges of QDs of different compositions.[2]

# IV.1.1. Synthesis of Quantum Dots

The first colloidal quantum dots were reported in 1983 by Brus *et col.*, who observed optical size effects for CdS nanocrystals grown in solution.[4] Since then, many scientists have focused their efforts on synthesizing new types of QDs. This section will be devoted to describe the synthesis of CdSe QDs, which have been the system of choice in this work. There exist two different kinds of CdSe nanocrystals: pure core CdSe QDs and core/shell QDs, whose CdSe core is capped with a layer of a different inorganic material. The following is a brief description of the synthesis of both types of CdSe QDs.

## IV.1.1.1. Synthesis of core CdSe quantum dots

Pure core CdSe nanocrystals are usually obtained by the method of hot injection, which was first introduced by Bawendi *et col.*[5] This methodology consists in heating a cadmium precursor (typically, CdO) in a solution of an organic stabilizer (e.g. oleic acid, OA) and a non-coordinating solvent such as 1-octadecene (ODE). When the mixture reaches a high temperature (*ca*. 300 ºC), the metal precursor decomposes and forms soluble cadmium-salts (e.g. $Cd(OA)_2$). Then, a previously prepared trioctylphosphine-Se complex (TOPSe) is added and, as depicted in Scheme IV-1, formation of CdSe nuclei takes place, which subsequently grow into the desired stabilizer-capped nanocrystals.[6]

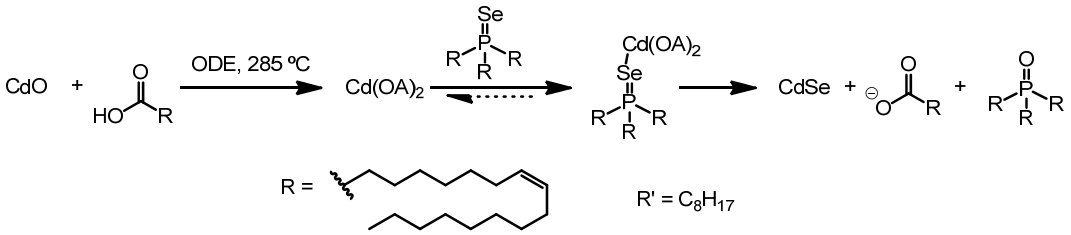


**Scheme IV-1.** Mechanism of formation of oleic acid-capped CdSe quantum dots as described by Liu *et al.*[5]

Even though core CdSe nanocrystals have been widely studied, they often present low photoluminescence quantum yields (PLQY) due to surface defects. Such defects are ascribed to the lower coordination number of surface atoms, which therefore exhibit unbounded orbitals. As a result, lower energy states than the LUMO energy level of QDs are created on their surface (the so-called "trap states"), where the exciton is trapped and relaxes back to the ground state via non-radiative mechanisms such as thermal dissipation, decreasing their photoluminescence.[7] Core passivation with a wider-bandgap inorganic shell prevents this phenomenon and produces more structurally stable and higher luminescent quantum dots.[8] In the case of CdSe QDs, the most common passivation shells are made of ZnS, thus giving rise to core/shell CdSe/ZnS nanocrystals.

## IV.1.1.2. Synthesis of core/shell CdSe/ZnS quantum dots

CdSe/ZnS QDs were firstly synthesized through a two-step process by Hines *et al.*, who overcoated CdSe QDs with one or two monolayers of ZnS.[8b] Those monolayers were grown by the addition of organometallic Zn and S precursors (e.g. diethylzinc and bis(trimethylsilyl)sulfide) to a hot solution of CdSe QDs previously prepared, which resulted in the formation of core/shell structures displaying impressive PLQY at that time (~50%). This was due to the protective role played by the ZnS shell introduced, which provided a physical barrier between the optically active core and the surrounding medium. As such, it did not only passivate surface trap states, but it also made CdSe cores less sensitive to surface chemistry and environmental influences.

Inspired by this precedent, new optimized methods for the preparation of core/shell nanocrystals have been reported since then.[1] In this work we have followed the synthetic strategy reported by Bae *et al.* in 2008, which produces highly luminescent CdSe/ZnS QDs in organic media by means of a simpler, one pot procedure.[9] This method relies on the faster crystallization rate of CdSe with respect to ZnS,[10] which allows the growth of CdSe-enriched cores and ZnS-enriched shells from a precursor mixture of both compounds. The synthesis starts with the heating of cadmium and zinc metal precursors (eg. CdO and $Zn(OAc)_2$) and organic stabilizers (eg. OA) dissolved in a non-coordinating solvent such as ODE. Then, a mixture of trioctylphophine-Se and S (TOP-Se and TOP-S) complexes is rapidly injected and the reaction is allowed to proceed at high temperature until reaching the desired nanocrystal size. Upon cooling down, core/shell CdSe/ZnS QDs are finally obtained by precipitation and centrifugation.[9]

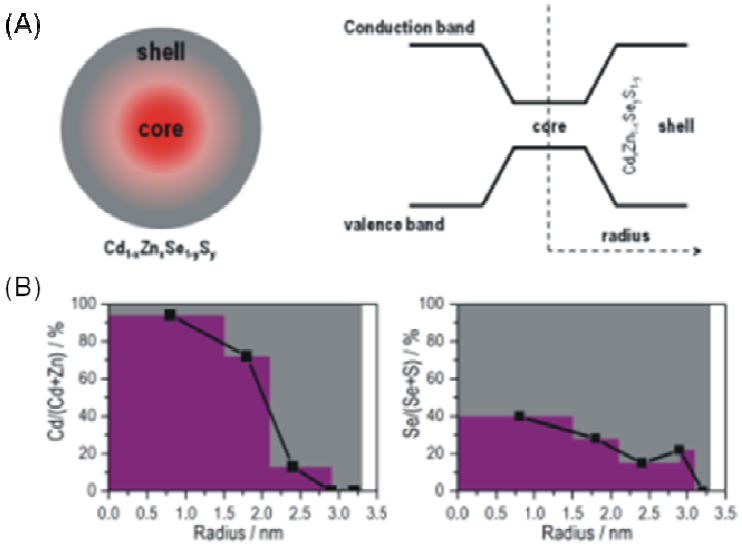


**Figure IV-2.** (A) General view of the internal structure and the energy band structure of this type of QDs. (B) Distance-dependent composition of a red emitting core/shell CdSe/ZnS QD ($Cd_{0.3}Zn_{0.44}Se_{0.22}S_{0.4445}$, reaction time= 5 min, $\lambda_{Em}$= 600 nm, and diameter=6 nm).[9]

It is important to note that this experimental procedure does not allow the formation of pure CdSe cores overcoated with pure ZnS shells. Instead, nanocrystals displaying a composition

gradient are obtained. As shown in Figure IV-2B, CdSe particularly concentrates in the inner core of the material and its content decreases with the distance from the center of the QD.

Contrarily, the ZnS distance-dependent profile follows an opposite trend, thus giving rise to hybrid structures resembling those of pure core/shell CdSe/ZnS QDs. In contrast to them, however, the size of the CdSe-enriched cores obtained and, therefore, the optoelectronic properties of the resulting composition gradient CdSe/ZnS QDs do not depend on reaction time but mainly on the chemical composition of the precursor mixture. In spite of this and their slightly different internal structures, from now on we will refer to composition gradient nanocrystals as core/shell CdSe/ZnS QDs for sake of simplicity.

## IV.1.2. Properties and applications of quantum dots

As already commented, QDs present unique optoelectronic properties that make them a promising alternative to standard organic fluorophores in many fields. Different factors account for this potential features:[1-3]

1. Owing to the inorganic nature of their optically active core, QDs are less prone to photo-oxidation and, therefore, more photostable than organic fluorophores.
2. As a result of quantum confinement effects, QDs present narrow photoluminescence spectra that can be finely tuned by changing the nanocrystal size (i.e. by simply controlling reaction time for pure core and pure core/shell nanocrystals). Quantum confinement is observed in semiconductors with sizes smaller than their exciton Bohr radii (typically, smaller than 10 nm). At these sizes, several effects take place: (a) exciton radiative recombination is favored; (b) the density of electronic states, which in the bulk material is nearly infinite, goes down to a few quantized energy levels; and (c) the energy of these electronic states and, therefore, of the optical bandgap of the material becomes very sensitive to the size of the system. As such, radiative relaxation from the first electronic excited state of QDs gives rise to photon emission in a narrow, symmetric and size-dependent energy band.[11]
3. Being of nanometer dimensions, QDs present a large surface-to-volume ratio. Together with its chemical nature, this allows functionalization of its outer layer with a large density of organic molecules in a rather straightforward manner. Such molecules are not only responsible of the colloidal stability of QDs, but also play an important role in their surface chemistry. Actually, the ability to exchange and modify the organic layer coating the nanocrystals has emerged as a key tool to link those nanoparticles to other surfaces[12] and biomolecules[13] for practical applications.

Because of their exceptional and tunable optoelectronic properties and versatile surface chemistry, QDs have emerged as a new family of nanomaterials for a number of applications, such as bioimaging,[14] quantum-dot-based light emitting diodes (QD-LEDs)[15] and quantum-dot-based solar cells (QD-SC) for photovoltaics.[16] In some of these applications, the preparation of controlled aggregates of QDs with different bandgaps is highly desired to exploit synergic effects, such as

unidirectional energy and/or electron transfer. For instance, this is the case of the so-called *rainbow solar cells*, a new generation of solar cells where the size-organization of QD aggregates on the nanoscale has enabled higher photoconversion efficiencies than for a tandem organization of QDs.[16] The development of a novel methodology to achieve the fabrication of such well-organized QD aggregates by means of covalent bonds is the main objective of this chapter.

## IV.1.3. Aggregates of quantum dots

To date a large volume of studies describing QD aggregation onto solid supports has been published, which make use of different methodologies such as direct deposition,[17] layer-by-layer deposition[18] chemical bath deposition[19] or electrophoretic deposition.[16a] These techniques can produce thin films of different QDs by sequential deposition of the nanocrystals; however, they do not allow the formation of discrete, colloidal heteroaggregates with defined interactions and separation distances between distinct QDs. Despite of their relevance for the preparation of nanometer-sized QD-based devices, reports on the preparation of such type of assemblies are much more scarce. Next, we introduce the most relevant examples described.

The simplest approach reported to date is the use of ditopic organic ligands that can be attached simultaneously to two different QDs, thus bringing them together into QD homoaggregates.[20] For instance, Peng *et al.* described the cross-linking of thiol-passivated CdSe nanocrystals by addition of a bis(acylhydrazide), which allowed the formation of the first reported colloidal homodimers of CdSe (Figure IV-3A).[20a] More recently, a similar approach was reported by Xu *et al.* to prepare analogous QD assemblies by means of a tetracarboxylic ligand (Figure IIV-3B).[20c]

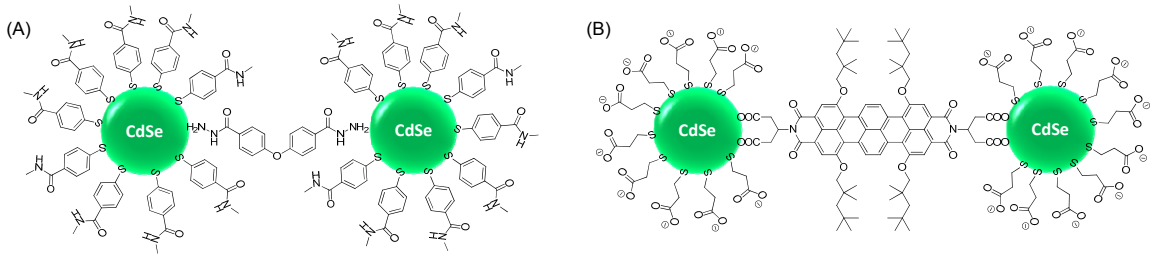


**Figure IV-3.** Homodimers of QDs prepared by addition of ditopic ligands: (A) bis(acylhydrazide) [20a] and (B) tetracarboxylic terrylendiimide derivative.[20c]

In spite of the success of this approach, it presents a severe limitation: the covalent assembly of QDs using ditopic ligands is not selective and, as a consequence, it does not allow different types of QDs to be linked together in a controlled manner. So far, this has only been achieved exploiting supramolecular interactions. In particular, two types of supramolecular interactions have been mainly explored to reach this objective: coloumbic ion-ion interactions[21] and molecular recognition between complementary ssDNA chains.[22]

In 2008, Gross *et al.* prepared heteroaggregates of CdSe and CdTe nanocrystals coated with thioglycolic acid (TGA),[21a] whose carboxylic group is deprotonated at low pH values. Addition of divalent calcium cations to a mixture of TGA-capped CdSe and CdTe QDs therefore caused spontaneous aggregation driven by coloumbic interactions. In this case, however, non-specific formation of homo- and heteroaggregates was observed, since both types of nanocrystals used presented negatively charged surfaces. (Figure IV-4A). To overcome this problem and selectively induce heteroaggregation, Wu *et al.* used QDs with oppositely charged capping ligands , as shown in Figure IV-4B.[21b]

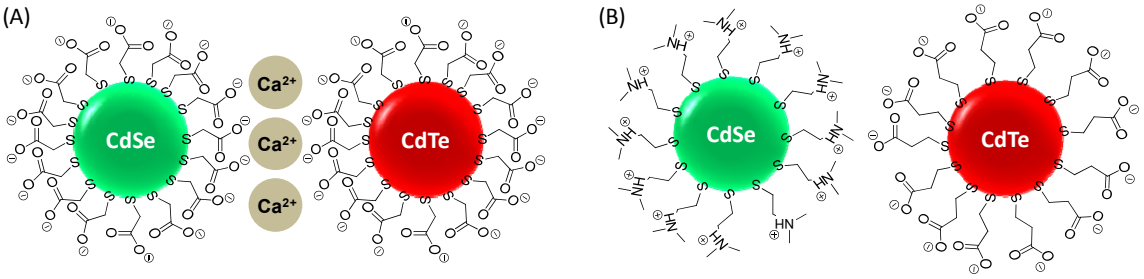


**Figure IV-4.** Schematic representation of QD aggregates formed by means of ion-ion interactions between (A) negatively-charged nanocrystals and divalent $Ca^{2+}$ ions,[21a] and (B) oppositely charged nanocrystals.[21b]

An alternative approach to electrostatic interactions was introduced in 2011 by Tikhomirov *et al.*, who exploited the recognition and self-assembly of complementary ssDNA chains tethered to the surface of different QDs to produce well defined QD heteroaggregates (Figure IV-5).[22] With this aim, they coated CdTe nanocrystals with mercaptopropionic acid and a controlled number ($n$ = 1-5) of functional ligands consisting of three different domains: (a) a phosphorothioate guanine oligonucleotide for QD binding; (b) a phosphodiester guanine oligonucleotide as spacer; and (c) a ssDNA sequence for QD aggregation. In this way, binary and even ternary supramolecular complexes with defined shapes and number of nanocrystals could be prepared. Later on, a similar DNA-based strategy was applied for the formation of homoaggregates of QDs.[23]

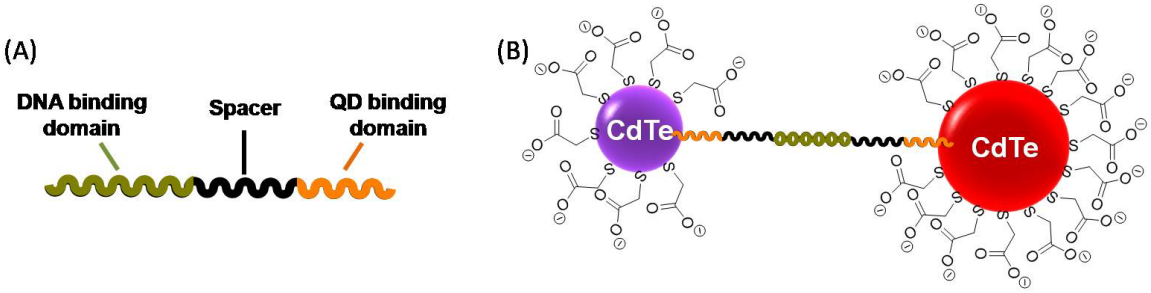


**Figure IV-5**. (A) Functional ligands used by Tikhomirov *et al.* for the construction of QD aggregates, which consist of three different domains. (B). QD supramolecular assemblies formed upon recognition of complementary ssDNA chains.[22]

Even though some of the precedents described report the successful formation of QD heteroaggregates, to date there are no examples in the literature of the preparation of such systems via covalent bonding. In view of this and the larger stability expected for this type of QD assemblies, we propose herein a new methodology to covalently tether different semiconductor nanocrystals in a controlled manner by means of a variant of the well-known azide-alkyne cycloaddtion (AAC) reaction.

## IV.1.4. Strain-promoted azide-alkyne cycloaddition

An azide-alkyne Huisgen cycloaddition (AAC) is a [3+2] cycloaddition reaction between an azide (which plays the role of the 1,3-dipole) and an alkyne (which acts as the dipolarophile) that leads to the 5-membered ring triazole (Figure IV-6). This is a regiospecific and concerted reaction that requires thermal activation.[24] The corresponding cupper-catalyzed azide-alkyne cycloaddition features an enormous rate increase (ca. $10^7$- to $10^8$-fold) compared to the uncatalyzed cycloaddition process at room temperature,[25] which combined to its high yield, wide scope, and lack of by-product formation has made this reaction one of the most exploited in click chemistry for the covalent tethering of functional fragments.

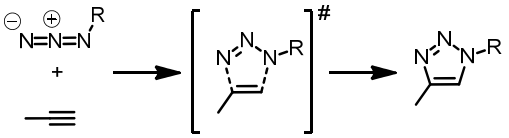

**Figure IV-6.** Schematic representation of a thermal azide-alkyne cycloaddition.

Indeed, the use of Cu(I)-catalyzed AAC for QD assembly has already been reported by Janczewski *et al.*, who produced homoaggregates of semiconductor nanoparticles coated with polymeric stabilizers bearing terminal azide and alkyne moieties.[26] Although the authors observed very efficient QD aggregation processes, the presence of traces of the catalyst resulted in a remarkable decrease of the photoluminescence intensity of the nanocrystals. As an alternative, Agard *et al.* developed the new strain-promoted azide-alkyne cycloaddtion (SPAAC) by using a *strained* alkyne (cyclooctyne), which *promotes*, spontaneously, the cycloaddition reaction at room temperature (Figure IV-7).[27] This specially favors the application of azide-alkyne cycloaddition in living cells, since it prevents the use of toxic cupper ions and the thermal denaturalization of proteins caused during thermal activation of regular AAC.

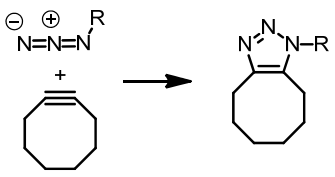

**Figure IV-7.** Schematic representation of the SPAAC reaction developed by Agard *et al.*[27]

Some important factors must be taken into account regarding this reaction:[28] (a) SPAAC (and AAC) proceed by reaction between two highly reactive groups compatible with most organic moieties; (b) SPAAC (and AAC) involves the lowest unoccupied molecular orbital (LUMO) of the cycloalkyne and the highest occupied molecular orbital (HOMO) of the azide; therefore, introducing electrowithdrawing groups (EWG) into the cyclooctyne ring accelerates the reaction rate (Figure IV-8A); and (c) as a particular case of thermal AAC, SPAAC leads to the formation of two different regioisomers with nearly equivalent yields for asymmetric cycloalkyne substrates. In the case of propargylic substituted cyclooctynes, these are the 1,4- and 1,5-regioisomers arising from transition states where the substituent of the azide lies in the same half-space than the substituent of cyclooctyne, or the opposite, respectively (Figure IV-8B).[a]

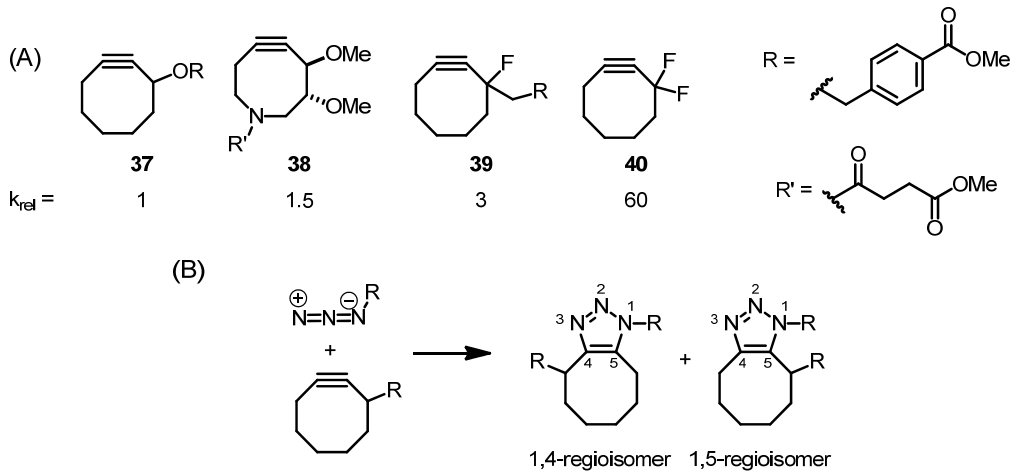


**Figure IV-8.** (A) Second-order rate constants of SPAAC between benzyl azide and several different cyclooctynes at room temperature. Noticeably, no reaction was observed between benzyl azide and non-strained acetylene under the same conditions.[27] (B) 1,4- and 1,5-regioisomers obtained from SPAAC for propargylic substituted cyclooctynes.

The capability of SPAAC to promote efficient Cu-free azide-alkyne cycloadditions has already been exploited in the functionalization of the organic capping layer of QDs, such as in the QD-labeling of biomolecules for *in vivo* imaging. As shown in Figure IV-9, Bernadin *et al.* functionalized the surface of CdSe/ZnS QDs with cyclooctyne **41** and then incubated CHO (Chinese Hamster Ovary) cells bearing azido-tagged mannosamine (ManNAz) in their membrane with the resulting nanocrystals. After 4h at 4 ºC, QDs were successfully covalently linked to the cell surface, as demonstrated by means of fluorescence microscopy.[29]

[a] Numbering of both regioisomers is based on triazole nomenclature (see Figure IV-8B).

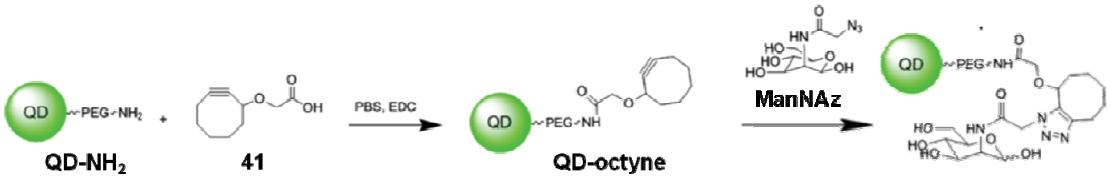


**Figure IV-9.** Schematic representation of the SPAAC reaction carried out by Bernadin *et al.* to covalently tether CdSe/ZnS QDs to the membrane of CHO cells exposing azido-tagged mannosamine towards the extracellular medium.[29]

This report demonstrates compatibility between SPAAC and QDs as well as proves that high reaction efficiencies can be achieved in azide-alkyne cycloadditons at room temperature without Cu-catalysis. Thus, SPAAC should be a good candidate for the construction of discrete, covalently-linked QD heteroaggregates. To demonstrate the viability of this methodology to accomplish this goal is the main objective of this chapter. Therefore, we propose herein the synthesis of different functionalized capping ligands for QDs and their use to promote for the first time controlled QD assembly via strain-promoted azide-alkyne cycloaddtion. The morphology and optical behavior of the resulting covalently-bonded QD aggregates will then be investigated to assess the capability of the fabrication strategy introduced in this work to allow the preparation of future QD-based photonic nanowires. These systems, which are inspired by the elegant operation of light-harvesting antennae in photosynthetic complexes,[30] should enable the efficient and unidirectional transport of electronic excitation energy on the nanoscale via non radiative energy transfer between close-by, energetically-ordered chromophores.

## IV.1.5. Preparation of quantum dots aggregates by SPAAC

Figure IV-10 shows a schematic representation of the strategy explored in this chapter for the preparation of discrete, covalently-linked QD heteroaggregates, which relies on the use of SPAAC between azide and cyclooctyne ligands. In particular, the key aspects of our approach are:

1. The design and preparation of four different ligands with proper functionalities capable of (i) tethering to the QD surface without detrimental effects on their optical properties (thiol and carboxylic acid moieties), and (ii) selectively reacting between them to give rise to nanocrystal assemblies (cyclooctyne and azide groups). In addition, a flexible, alkyl linker will be introduced between the two functional units of each ligand.
2. The synthesis of core CdSe and core/shell CdSe/ZnS semiconductor nanocrystals. As commented in the introduction, their absorption and emission spectra falling in the visible range make these QDs potential candidates for a number of different applications.
3. The replacement of the initial capping stabilizers of the QDs introduced during their synthesis by the functionalized ligands via ligand exchange procedures  This will be required by the high

temperatures needed for the synthesis of the semiconductor nanoparticles, which should therefore be undertaken with highly thermally stable ligands (e.g. oleic acid).

4. SPAAC assays between different QDs for the formation of discrete, covalently-linked heteroaggregates of QDs. In particular, two types of nanocrystal assemblies will be prepared (**M13** and **M14**) using distinct initial QDs and functionalities for ligand tethering to the semiconductor nanoparticles.
5. The characterization of the resulting QD heteroaggregates by NMR, transimission electron microscopy (TEM) and optical techniques to evaluate SPAAC as an efficient method for conducting nanocrystal assembly. This would then allow the application of such methodology for the construction of QD-based functional materials, such as photonic nanowires.

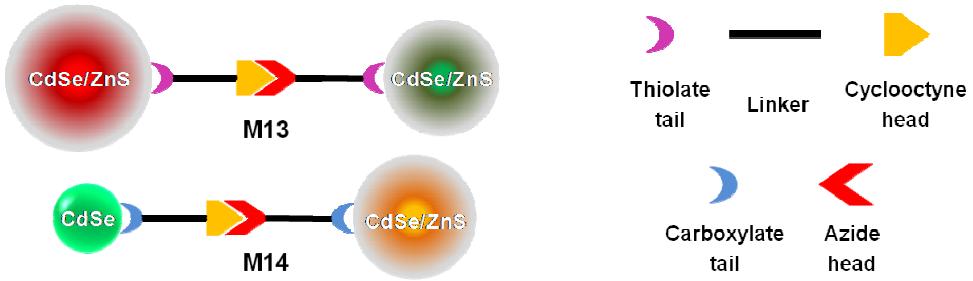


**Figure IV-10.** QD heteroaggregates (**M13** and **M14**) to be prepared in this work via SPAAC reaction between azide and cyclooctyne moieties tethered to the surface of CdSe and CdSe/ZnS nanocrystals through carboxylate and thiolate groups.

# IV.2. RESULTS AND DISCUSSION

## IV.2.1. Synthesis and characterization of ligands

Our novel approach for the preparation of convalently-linked QD assemblies relies on the occurrence of [3+2] cycloaddition reactions between azide and cyclooctyne moieties on the surface of the nanoparticles. Therefore, our first step towards this goal consisted in the synthesis of ligands bearing these reacting groups and appropriate functionalities for QD binding. In particular, the four ligands shown in Figure IV-11 were prepared: 11-azidoundecanoic acid, **42**, 11-azidoundecanethiol, **43**, 10-(cyclooct-2-yn-1-yloxy)decanoic acid, **44** and 11-(cyclooct-2-yn-1-yloxy)undecane-1-thiol, **45**. As previously mentioned, carboxylic acids and thiols were chosen as QD capping agents, which were selectively functionalized with azide and cyclooctyne reactive groups. For each ligand, both functional moieties were linked by a saturated alkyl chain of at least eight carbons to ensure (i) a compact organic layer onto the QD surface by van der Waals interactions, and (ii) enough

separation between the reactive groups and the QD surface to facilitate the approach of the azide and alkyne units. While the preparation of carboxylic azide **42**,[31] carboxylic cyclooctyne **44**,[32] and thiolated azide **43**[33] was already described in the literature, synthetic reports did not exist for thiolated cyclooctyne **45** at the beginning of this thesis. As explained below, the synthesis of this ligand was designed analogously to that reported for similar cyclooctyne **44**.

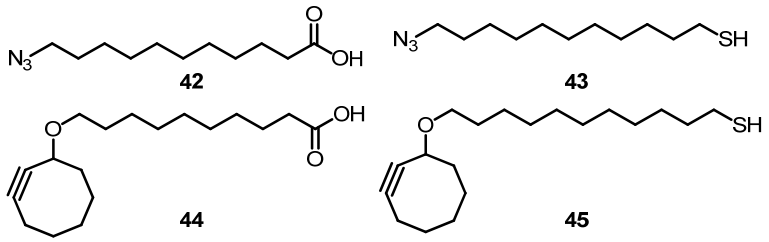


**Figure IV-11.** Target ligands to be exploited for QD covalent assembly by means of SPAAC.

## IV.2.1.1. Synthesis of 11-azidoundecanoic acid, 42

Azide **41** can be obtained from the commercial compound 11-bromoundecanoic acid, **46**, via nucleophilic substitution.[31] A well-known methodology to attain this goal implies the use of sodium azide as nucleophile in polar solvents (DMF or DMSO),[34] which guarantees the dissolution of both reactants in the reaction medium. To facilitate the subsequent treatment of the reaction mixture and isolation of the desired product by extractions with diethylether, DMF was chosen as solvent in our case. In this way, 11-azidoundecanoic acid was obtained nearly quantitatively (99 %, Scheme IV-2). Analysis by $^1$H NMR of this compound was in agreement with the data reported in the literature;[31] hence, it was used in subsequent ligand exchange studies without further purification.

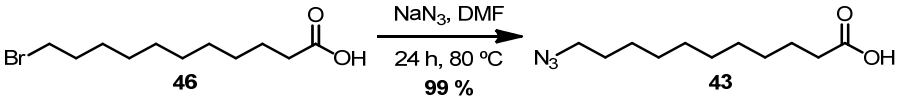


**Scheme IV-2.** Nucleophilic substitution reaction for the formation of target ligand **41**.

## IV.2.1.2. Synthesis of 11-azidoundecanthiol, 43

Although the preparation of compound **43** had already been reported,[33] a new synthetic pathway was designed in this work to obtain this compound in better yield. As shown in Scheme IV-3, this pathway relies on the sequential introduction of the desired functionalities into commercially available 11-bromoundecanol, **47**.

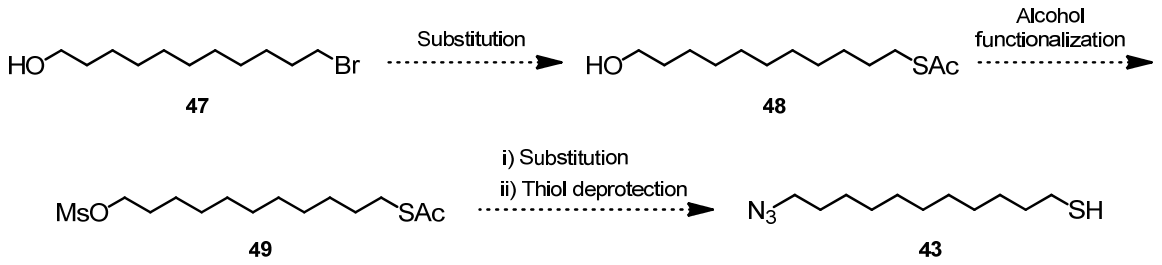


**Scheme IV-3.** Synthetic methodology designed for the preparation of ligand **43**.

Thus, our synthetic approach started with the nucleophilic substitution of the bromide of 11-bromoundecanol by thioacetate to yield intermediate **48** (Scheme IV-4). After consumption of the starting material as revealed by TLC, thioacetate **48** was isolated and obtained in high purity and quantitive yield by simple extractions. This was demonstrated by comparison of its $^{1}$H NMR spectrum with that previously described for this compound,[35] which was used in the next step without further purification.

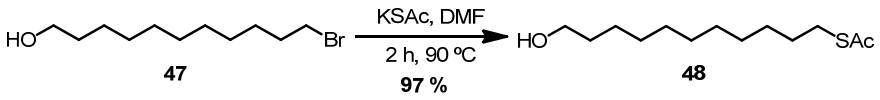


**Scheme IV-4.** Nucleophilic substitution of bromine by thioacetate group for the synthesis of intermediate **48**.

The introduction of the azide moiety into thioacetate **48** by nucleophilic substitution required previous transformation of its alcohol moiety into a better leaving group. Among the different ways developed to achieve this goal,[36] we undertook herein the conversion of the hydroxyl group to a sulphonate, as depicted in Scheme IV-5. Complete conversion of the starting material was observed after 10 h at our experimental conditions by means of TLC. Pure mesylate **49** was then isolated in quantitative yield from the reaction mixture and characterized by $^{1}$H NMR, $^{13}$C NMR, IR and HR-MS. The $^{1}$H NMR spectrum of this compound clearly confirms mesylate formation owing to the occurrence of a new signal at 3.00 ppm corresponding to the mesyl group introduced and the down-field shifts observed for the aliphatic protons in $\alpha$- and $\beta$-position with respect to the sulphonate.

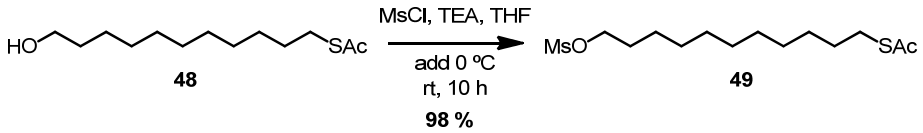


**Scheme IV-5.** Synthesis of intermediate **49** from alcohol **48**.

Next, compound **50** was prepared upon nucleophilic substitution of the mesyl moiety in **49** with sodium azide, using the same methodology previously applied to the synthesis of **42** (Scheme IV-6). Analysis by $^{1}$H NMR of the resulting product was in agreement with the reported data.[33]

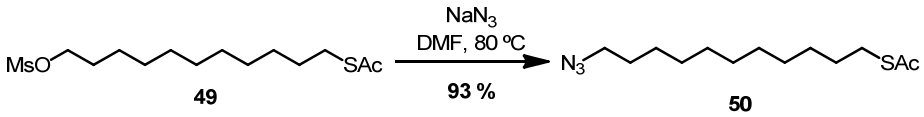


**Scheme IV-6.** Nucleophilic substitution carried out for the synthesis of intermediate **50**.

Finally, target ligand **43** was obtained by thioacetate cleavage of compound **50**, a reaction that can take place both in acid or basic conditions.[37] However, it must be taken into account that the use of basic conditions favors the formation of the corresponding disulfide dimers. By contrast, thioacetate hydrolysis under acidic conditions usually prevents this undesired reaction. For this reason, thiol deprotection of **50** was carried out under an excess of hydrochloric acid in refluxing MeOH (Scheme IV-7). In this way, compound **43** was obtained quantitatively and in high purity after the work up of the reaction mixture, as demonstrated by its $^1$H NMR spectrum.[38] The target azido-thiol ligand was therefore obtained in 4 steps and with an 88 % overall yield by means of the synthetic pathway devised in this work, which improves the results of the procedure previously reported for the preparation of this compound (4 steps, 60 % yield).[33]

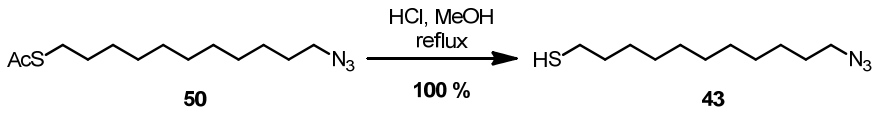


**Scheme IV-7.** Thioacetate cleavage reaction for the obtaining of target ligand **43**.

## IV.2.1.3. Synthesis of 10-(cyclooct-2-yn-1-yloxy)decanoic acid, 44

Cyclooctyne ligand **44** was synthesized according to the methodology described by Neef *et al*. (Scheme IV-8),[32] which starts from commercially available cycloheptene, **49**. Addition of dibromocarbene to this substrate should lead to bicyclic compound **52**, which, by the action of a Lewis acid, can originate the corresponding cyclopropyl cation and undergo the subsequent electrocyclic ring opening reaction to form cyclooctene **54** after final trapping by the selected nucleophile. Target cyclooctyne **44** would be finally synthesized from this intermediate via $\alpha$-vinylic elimination and carboxylic acid deprotection.

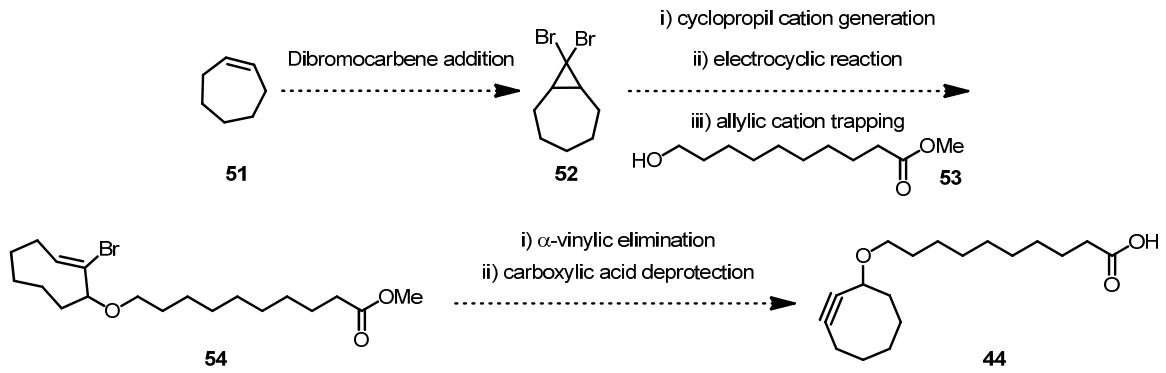


**Scheme IV-8.** Synthetic route reported by Neef *et al.* for the preparation of target ligand **44**.[32]

Addition of dihalocarbenes to alkene systems has been deeply studied since more than six decades.[37,39] In the case of dibromocarbene, it can be prepared *in situ* by treatment of bromoform with a bulky strong base,[40] and then added over a solution of the olefin of interest to promote the cycloaddition reaction. These conditions were applied in this work for the obtaining of byciclic product **52** with 71 % yield, in agreement with the results from Neef *et al.*[32] (Scheme IV-9).

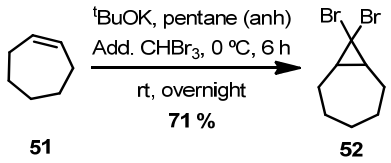


**Scheme IV-9.** Preparation of **52** from commercial cycloheptene.

Next, the preparation of cyclooctene **54** was performed using an electrocyclic ring opening reaction involving two π-electrons as key reaction. Reese *et al.* first reported $AgClO_4$-promoted ring expansion of 8,8-dihalobicyclo[5.1.0]octanes, which proceeds through the formation of an allyl cation intermediate that is subsequently captured by the nucleophiles in the reaction medium (Figure IIV-12).[41] Two different pathways are possible for this reaction depending on which bromine atom interacts with the silver cation and is eventually eliminated, thereby leading to two distinct products. Thus, elimination of the *exo*-bromine atom leads to a *trans,trans*-allyl cation[b] (**II**), which will then give rise to the resulting (*Z*)-bromocyclooctene derivative **IV**. On the other hand, elimination of the *endo*-bromine atom results in a *cis,cis*-allyl cation (**III**), which should next lead to the formation of the (*E*)-bromocyclooctene product **V**. Although formation of the *trans,trans*-allyl cation is expected to be faster because of the better accessibility of the *exo*-bromine atom, it can thermally isomerize to **III** and, as a consequence, a mixture of both cyclooctene products **IV** and **V** can be obtained. This is of high importance for the synthesis of the target cyclooctyne compound, since it must be formed via a stereospecific *anti*-elimination of the vinyl bromide moiety of **54**, which can only take place on the (*Z*)-cyclooctene isomer. This is therefore the desired product of the ring expansion reaction.

[b] In the notation used by Reese *et al.* for the intermediate allyl cations of the reaction, *trans* and *cis* refer to the relative configuration of hydrogen and bromine substituents.

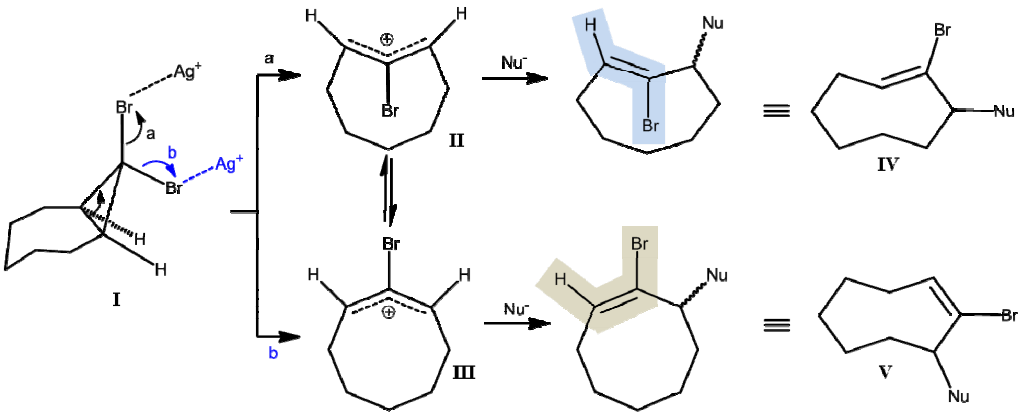


**Figure IIV-12.** Schematic representation of the two possible pathways for the $AgClO_4$-promoted ring expansion of 8,8-dibromobicyclo[5.1.0]octane (a = *exo* and b = *endo* ring opening).

In view of this, we applied the same reaction conditions described by Neef *et al.*, who reported the selective formation of (*Z*)-**54** in a rather good yield (61%) at room temperature by using a large excess of nucleophile **53** (10 eq), adding silver perchlorate to a previously prepared mixture of starting materials **52** and **53**, and conducting the reaction in the dark (Scheme IV-10). This should favor fast reaction of the *trans,trans*-allyl cations formed, therefore minimizing undesired isomerization to the *cis,cis*-intermediate.

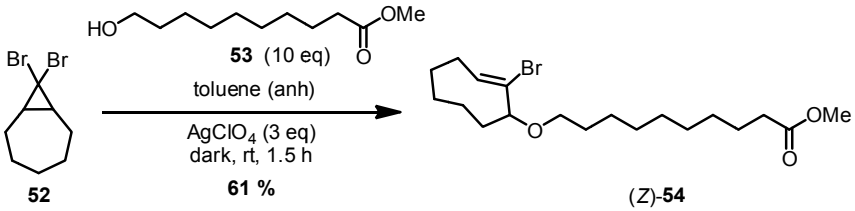


**Scheme IV-10.** Conditions used by Neef *et al.* for the synthesis of (*Z*)-**52**.[32]

Surprisingly, when testing these same reaction conditions, we did not observe the selective formation of (*Z*)-**54**, but an (*E*)-**54** enriched mixture of the two possible isomers (23:77 (*Z*)-:(*E*)-mixture; entry 1 in Table V.1). This was unambiguously confirmed by the $^1$H NMR spectrum of the crude material, which showed two different olefinic signals that were assigned using the reported data for (*Z*)-**54**: a triplet at 6.29 ppm and a double doblet at 6.17 ppm, which correspond to the olefinic proton of the (*E*)- and (*Z*)-isomers, respectively (Figure IV-13B).[41] Since all purification procedures attempted to separate this mixture of products (distillation, flash chromatography and preparative TLC) were unsuccessful and no other reports describing alternative conditions for the preparation of (*Z*)-**54** were found, the ring expansion reaction of bicyclic compound **52** was optimized.

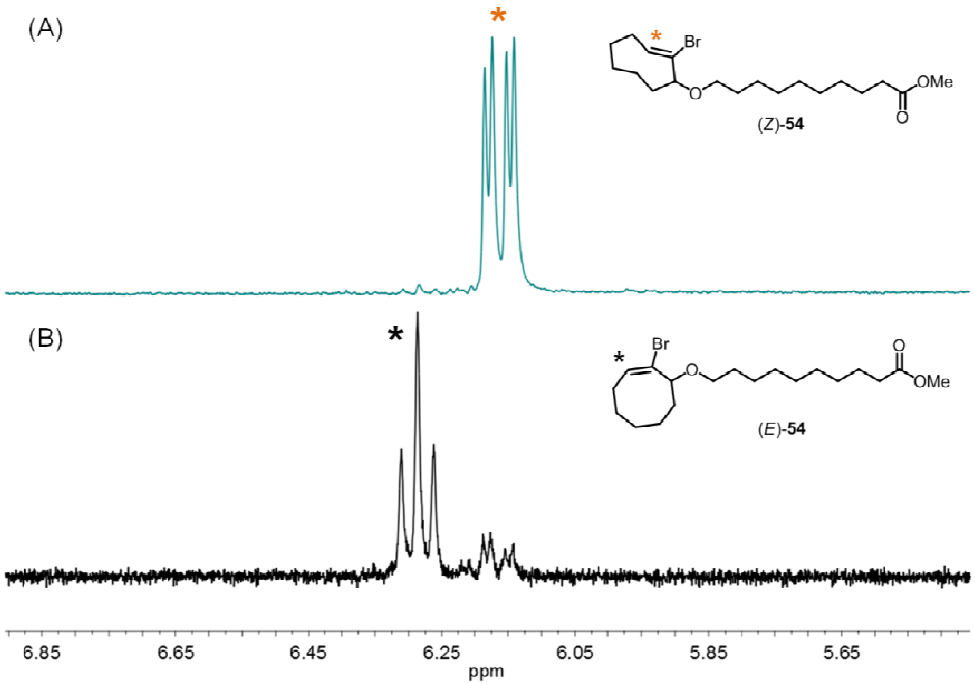


**Figure IV-13.** $^{1}$H NMR ($CDCl_3$, 400 MHz) spectra of the olefinic region of the product obtained from the ring expansion reaction of **52** using (A) the optimized conditions found in this work (see Table IV.1), and (B) the conditions reported by Neef et al.[32]

Several different experiments were undertaken to find the optimal conditions for the selective formation of (*Z*)-**54**, in which those reported from Neef *et al*. were rationally varied: (a) the order in which $AgClO_4$ and nucleophile **53** were added to the bicylcic substrate, since the first step of the reaction requires the use of silver ions; (b) the amount of excess nucleophile due to its high price; (c) the illumination conditions; (d) the temperature at which $AgClO_4$ is poured over **52** and the resulting mixture preserved prior to the addition of **53**. As shown in Table IV-1, all these parameters play an important role in the reaction, and the selective formation of the target (*Z*)-isomer was only observed when (i) $AgClO_4$ was first added over the starting material at low temperature (0 ºC), (ii) the formation of the resulting *trans,trans*-allyl cation was allowed to proceed for 15 min while minimizing undesired isomerization by maintaining the reaction mixture at this temperature in the dark, and (iii) a large excess of **53** (10 eq.) was subsequently introduced to rapidly capture the *trans,trans*-allyl intermediate at room temperature (Scheme IV-11). In this way, the formation of (*E*)-**54** was nearly suppressed, as clearly proven by the $^{1}$H NMR of the final product (Figure IV-13A).

**Table IV-1**. Experimental conditions assayed for the optimization of the electrocyclic reaction to selectively obtain target compound (*Z*)-**52**.

| | First reactant added | 53 (eq) | Illumination conditions | T $AgClO_4$ addition (ºC) | Yield (%) | (*Z*) : (*E*) ratio[a] |
|---|---|---|---|---|---|---|
| **1**[b] | **53** | 10 | darkness | rt | 40 | 23 : 77 |
| **2** | $AgClO_4$ | 3 | ambient light | rt | 54 | 10 : 90 |
| **3** | $AgClO_4$ | 10 | ambient light | rt | 58 | 64 : 36 |
| **4** | $AgClO_4$ | 10 | darkness | rt | 60 | 80 : 20 |
| **5** | $AgClO_4$ | 10 | darkness | 0 ºC | 62 | 100 : - |

[a] Determined by $^1$H NMR. [b] Conditions from reference [32].

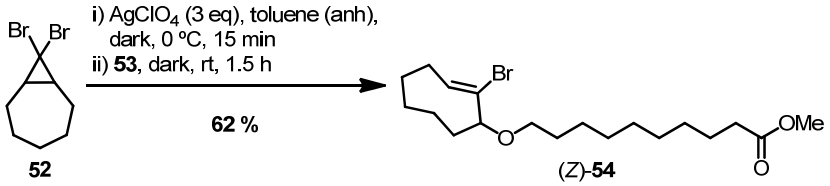


**Scheme IV-11.** Optimal conditions achieved in this work to selectively obtain desired (*Z*)-**52**.

After successfully preparing cyclooctene (*Z*)-**54**, we undertook the final steps for the synthesis of ligand **44**. This first required cyclooctene to cycloctyne conversion by treatment with a strong and non-nucleophilic base, which should abstract the olefinic proton of **54** and thus promote elimination of the bromine atom to obtain the target alkyne.[37] Similarly to bimolecular elimination E2 of alkyl bromides, this reaction is stereospecific and requires the vinylic proton and the bromine atom to be located in relative *anti* positions, as it is the case in (*Z*)-**54**. Following the methodology reported by Neef *et al.*,[32] we used in this work 1,8-diazabicycloundec-7-ene (DBU) as a strong and non nucleophilic base to promote the elimination of the vinyl bromide moiety of (*Z*)-**54**. The resulting cyclooctyne product was not isolated, but it was directly treated with aqueous NaOMe to deprotect its carboxylic group and obtain target ligand **44** quantitatively (Scheme IV-12), as confirmed by $^1$H NMR where the olefinic proton disappeared and H-1' signal shifted down-field from 3.81 to 4.14 ppm. From starting cycloheptene, this compound was prepared in 3 reaction steps with an overall yield of 37 % and it was subsequently used without further purification in ligand exchange processes for QD binding.

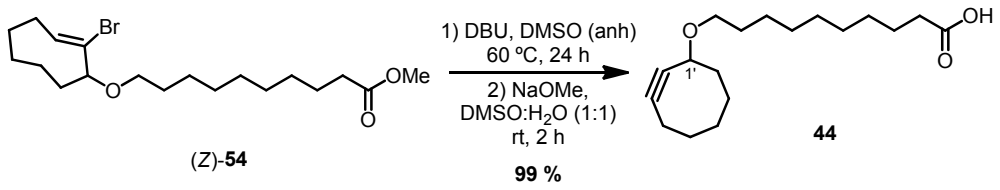


**Scheme IV-12.** Reaction conditions for the formation of target ligand **44**.

## IV.2.1.4. Synthesis of 11-(cyclooct-2-yn-1-yloxy)-undecanethiol, 45

The synthetic route for the formation of ligand **45** was designed to be as similar as possible to that already assayed for the synthesis of **44** (Scheme IV-13). Thus, it also started from commercial cycloheptene, which would be similarly modified via dibromocarbene addition and electrocyclic ring opening reaction. In the latter step, a different nucleophile, 11-bromoundecanol, would be used for capturing the allylic cation, thus obtaining the (*Z*)-cyclooctene intermediate **55** whose alkylbromide group would be converted into thioacetate **56**. Ligand **45** would be finally synthesized from this compound after vinylic elimination of the olefinic bromine atom and deprotection of the thiol group.

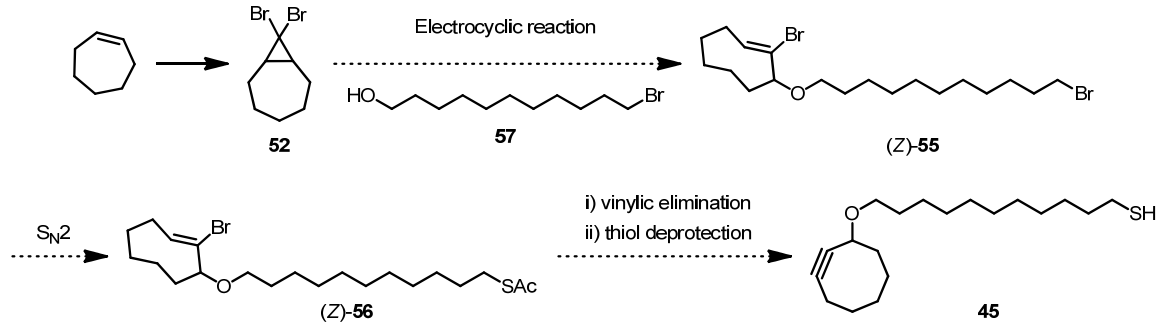


**Scheme IV-13.** Synthetic route planned for the obtaining of target ligand **44**.

The preparation of cyclooctene (*Z*)-**55** was attempted following the same synthetic methodology optimized for the formation of (*Z*)-**54**. In this case, commercially available 11-bromoundecanol was used as nucleophile in the electrocyclic ring opening reaction with bicyclic compound **52** (Scheme IV-14). In this way, the desired cyclooctene (*Z*)-**55** was selectively obtained in 62% with no traces of formation of its (*E*)-isomer, and it was next characterized by $^{1}$H NMR, $^{13}$C NMR, IR and HR-MS.

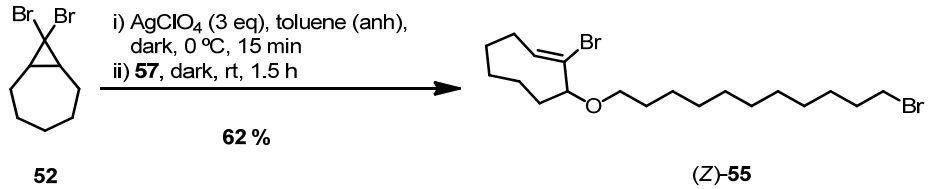


**Scheme IV-14.** Electrocyclic reaction for the synthesis of compound (*Z*)-**55**.

Nucleophilic substitution of the terminal bromine atom of (*Z*)-**55** with potassium thioacetate was then attempted to prepare (*Z*)-**56** using similar conditions to those previously applied in the synthesis of ligands **42** and **43** (Scheme IV-15). However, when the same conditions were assayed, isomerization of the cyclooctene moiety was observed and first attempts yielded a mixture of both (*Z*)- and (*E*)-**56**. Although the actual mechanism of the process is not clear to us, we ascribed this result to the presence of an excess amount of thioacetate. Accordingly, we only used 1.2 equivalents of KSAc in further experiments to avoid cyclooctene isomerization. After 2 h of reaction and purification by extraction processes, thioacetate (*Z*)-**56** was selectively obtained in 76 % yield and fully characterized. Formation of this product could be evidenced by $^{1}$H NMR: a new singlet

signal corresponding to the thioacetate group introduced was observed at 2.32 ppm, while the triplet signal from H-11' shifted up-field from 3.40 ppm to 2.86 ppm.

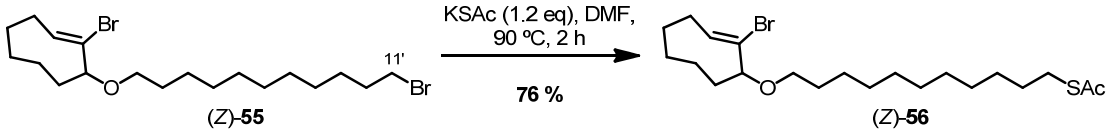


**Scheme IV-15.** Nucleophilic substitution reaction for the incorporation of the thioacetate moiety in (*Z*)-**55**.

Next, the same conditions used in the final step of the synthesis of ligand **44** were applied to the formation of cyclooctyne **45** from (*Z*)-**56**, which should proceed via elimination of its vinyl bromide moiety and hydrolysis of its thioacetate group in a stepwise manner using basic media (Scheme IV-16). However, two main differences were observed when applying the same reaction conditions to (*Z*)-**56**: (a) the desired thiol group was not obtained upon thioacetate cleavage with aqueous NaOMe, but it further reacted under the basic conditions used to form the corresponding disulfide dimers, as shown in Scheme IV-16; and (b) in spite of all precautions taken, partial isomerization of the initial cyclooctene substrate to its *E*-isomer was observed, which did not undergo the elimination reaction to give the desired cyclooctyne compound. Instead, it suffered thioacetate cleavage followed by disulfide formation at our experimental conditions. As a result, a complex and irreproducible mixture (resolved by HR-MS) of homo- and heterodimers **58**, **59** and **60** was finally obtained.

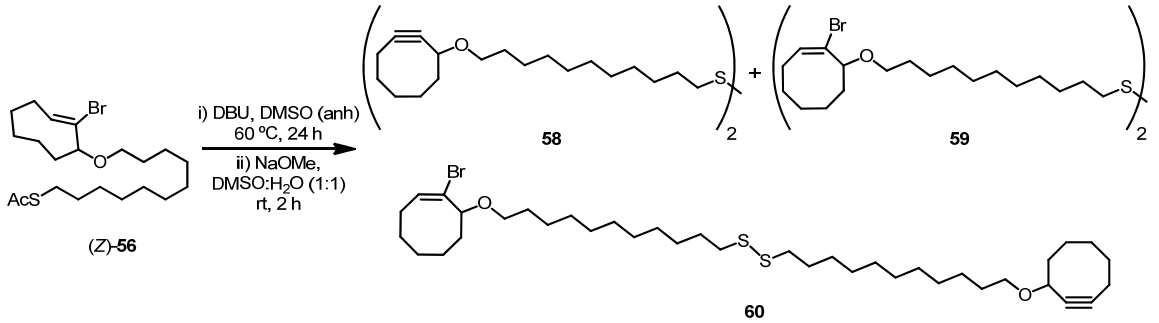


**Scheme IV-16.** Mixture of products formed when attempting the $\alpha$-vinylic elimination and thioacetate cleavage reactions of (*Z*)-**56**.

Separation of these compounds by flash chromatography, preparative TLC or distillation at reduced pressure was totally unsuccessful, and only a very minor fraction of pure compound **58** could be isolated once and properly characterized. In addition, all our initial efforts to minimize the isomerization of the initial (*Z*)-cyclooctene and, therefore, the formation of **59** and **60** also failed, which involved lowering the reaction temperature down to rt, reducing the reaction time, and changing the base used to promote the elimination reaction. A detailed investigation of this reaction revealed that partial thioacetate cleavage already took place during the treatment with DBU, probably due to the presence of some water traces in the reaction medium. Thiol oxidation and formation of sulfur radical species were then expected to occur, which might be the responsible to induce the cyclooctene isomerization process provided that the same temperature and illumination

conditions used in this case did not cause any effect on non-thiolated substrate (*Z*)-**54** (see section V.2.1.3). Nevertheless, DBU anhidrization and oxygen removal to prevent radical formation did not completely suppress cyclooctene isomerization and, in the best case, a 5.8:1 mixture of target cyclooctyne and undesired (*E*)-cyclooctene units was obtained.[c] This was confirmed by $^1$H NMR, which showed distinguishable signals for both groups (Figure IV-14A): (a) a multiplet at 4.15 ppm assigned to the propargylic proton of the cyclooctyne ring, as well as the two double triplets at 3.54 and 3.29 ppm corresponding to the diastereotopic α-protons of its alkoxy sidechain; and (b) two triplets at 6.30 and 4.30 ppm attributed to the olefinic and allylic protons of the (*E*)-cyclooctene moiety, respectively, and two additional triplets at 3.63 and 3.41 assigned to the diastereotopic α-protons of the alkoxy substituent. No differences were instead observed for the signals of the protons at the α-position with respect the disulfide bond, which for the three products in the mixture overlapped and fell at 2.67 ppm.

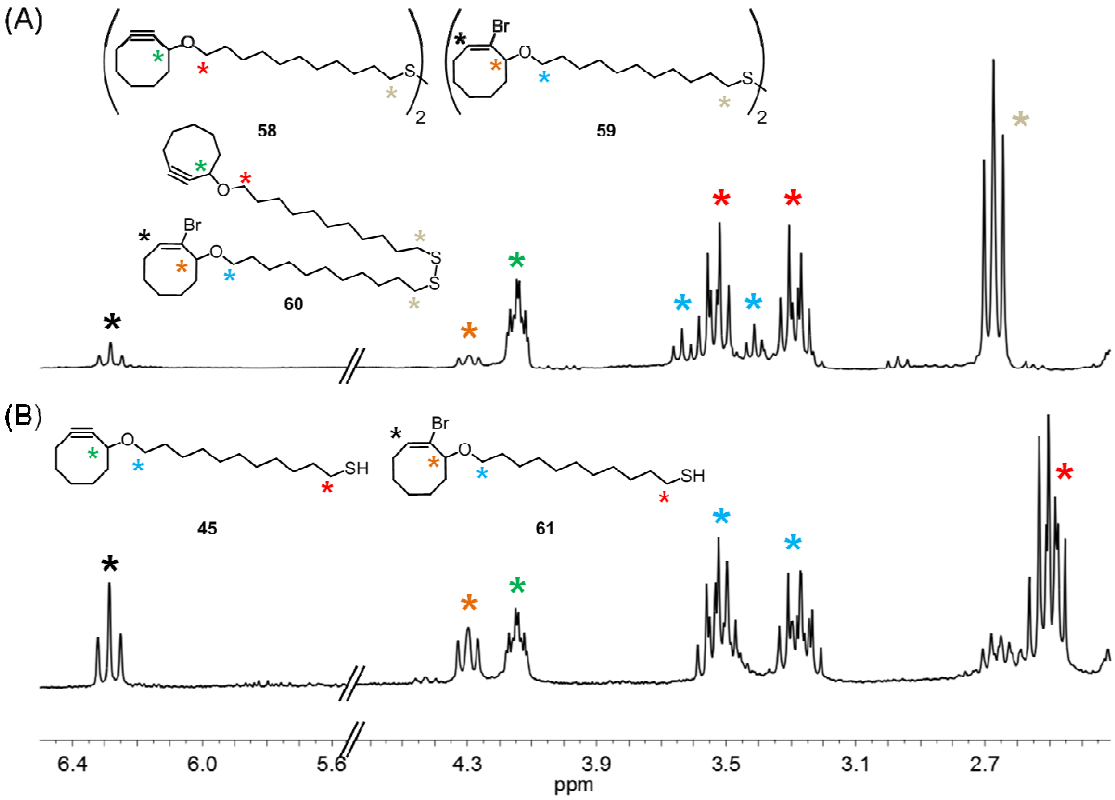


**Figure IV-14.** $^1$H NMR ($CDCl_3$, 400 MHz) spectra of the most remarkable signals of (A) the mixture of disulfide dimers **58**-**60** obtained after vinylic elimination and thioacetate cleavage of (*Z*)-**56**, and (B) the mixture of thiols **45** and **61** generated by reduction of the dilufide bonds of **58**-**60**.

As an alternative way to selectively isolate desired cyclooctyne **45**, we attempted to resolve the complex mixture of products obtained by performing the separation process after cleavage of the

[c] Yield could not be determined due to the presence of a ternary mixture of compounds with identical signals in $^1$H NMR spectrum.

disulfide bridges. With this aim, a mixture of compounds **58**-**60** was first reacted with $PBu_3$ in MeOH at 0 ºC (Scheme IV-17), a methodology that reduces disulfide bonds[42] without affecting alkynes.[43] Then, different separation procedures were tested for the new mixture of compounds **45** and **61** prepared. Unfortunately, unsuccessful results were again obtained by flash chromatography, preparative TLC and distillation at reduced pressure, and a 1.37:1 mixture of cyclooctyne **45** and cyclooctene **61** was isolated in the best case, with 45 % yield for ligand **45**, from a starting mixture of **58**-**60** with a cyclooctyne/(*E*)-cyclooctene ratio of 1.5:1. Figure IV-14B shows the $^1$H NMR spectrum of this mixture, where separate sets of signals are observed for both products. Noticeably, the most significant spectral differences found with respect to the starting materials **58**-**60** were the change in multiplicity (from triplet to quartet) and up-field shift (from 2.67 to 2.45-2.60 ppm) of the signals corresponding to the methylene group that holds the sulfur-containing group.

In addition to uncompleted separation from undesired cyclooctene **61**, ligand **45** was also found to be rather unstable. Thus, 28 % conversion into a new product was observed after one week even when stored at -18ºC in the dark. Although we did not attempt to characterize this new compound, we ascribe it to a cyclooctene sulfide derivative of ligand **45** due to an inter- or intramolecular thiol-yne addition as it is reported in the literature.[44] In view of this, we decided to store ligand **45** as the more stable, protected disulfide **58**, which was obtained in 4 steps, 4 % overall yield and as a non-resolvable mixture with compounds **59** and **60**. This mixture was reduced to the corresponding thiol derivatives **45** and **61** only when needed for QD functionalization and used immediately without further purification. Although it may also tether to the QD surface during ligand exchange processes, cyclooctene **61** is expected not to interfere in the subsequent experiments aiming at controlled QD assembly by means of SPAAC.

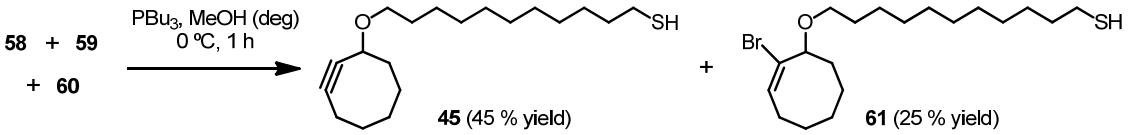


**Scheme IV-17.** Mixture of thiols obtained by reduction of the disulfide bonds of **58**-**60**.

## IV.2.2. Synthesis of QDs and ligand exchange studies

As commented in the introduction of this chapter, different types of QDs were synthesized in order to prepare convalently-linked heteroaggregates. In particular, we tuned the composition (CdSe and CdSe/ZnS) and sizes of the QDs to (i) modulate their optical properties, and (ii) enable selective identification of the nanocrystals in the final assemblies of QDs. Once prepared, the organic stabilizers of their capping layer were exchanged with functional ligands **42**-**45** to allow subsequent QD aggregation by SPAAC.